A reinforcement learning guided hybrid evolutionary algorithm for the latency location routing problem

Yuji Zou [a], Jin-Kao Hao [a,*] Qinghua Wu [b,*]

[a] *LERIA, Université d'Angers, 2 Boulevard Lavoisier, 49045 Angers, France*

[b] *School of Management, Huazhong University of Science and Technology, No. 1037, Luoyu Road, Wuhan, China*

Computers & Operations Research, July 2024
https://doi.org/10.1016/j.cor.2024.106758

Abstract

The latency location routing problem integrates the facility location problem and the multi-depot cumulative capacitated vehicle routing problem. This problem involves making simultaneous decisions about depot locations and vehicle routes to serve customers while aiming to minimize the sum of waiting (arriving) times for all customers. To address this computationally challenging problem, we propose a reinforcement learning guided hybrid evolutionary algorithm following the framework of the memetic algorithm. The proposed algorithm relies on a diversity-enhanced multi-parent edge assembly crossover to build promising offspring and a reinforcement learning guided variable neighborhood descent to determine the exploration order of multiple neighborhoods. Additionally, strategic oscillation is used to achieve a balanced exploration of both feasible and infeasible solutions. The competitiveness of the algorithm against state-of-the-art methods is demonstrated by experimental results on the three sets of 76 popular instances, including 51 improved best solutions (new upper bounds) for the 59 instances with unknown optima and equal best results for the remaining instances. We also conduct additional experiments to shed light on the key components of the algorithm.

Keywords: Routing; Latency location routing; Cumulative capacitated vehicle routing; Heuristics; Learning-driven optimization.

* Corresponding author.
Email addresses: yujizou6@gmail.com (Yuji Zou), jin-kao.hao@univ-angers.fr (Jin-Kao Hao), qinghuawu1005@gmail.com (Qinghua Wu).

1 Introduction

The location routing problem (LRP) plays a critical role in logistics management. The problem can be viewed as consisting of two sub-problems: the facility location problem FLP (i.e., selecting which depots to open) and the multi-depot vehicle routing problem (i.e., minimizing travel distance or other distance-related costs). The complexity of this problem arises from the need to consider both sub-problems simultaneously. The latency location routing problem (LLRP) is a LRP variant where the objective function of the underlying routing problem is to minimize the total waiting time of all customers. This customer-centric problem has many applications in different contexts related to emergency logistics operations in post-disaster relief, last-mile delivery with shared intermediate facilities in urban logistics, and delivery of perishable products (Ngueveu et al., 2010; Nucamendi-Guillén et al., 2022).

The LLRP can be thought of as a combination of the FLP and the multiple depot cumulative vehicle routing problem (MDCCVRP). Given that both constituent problems are NP-hard, the LLRP is inherently a computationally challenging problem (Moshref-Javadi & Lee, 2016). The problem can be defined on a directed complete graph $G = (V, E)$ with $V = D \cup C$ and $E = \{(i, j) : i, j \in V, i \neq j\}$, where D is the set of homogeneous uncapacitated depots ($|D| \geq 1$) and $C = \{C_1, C_2, ...C_m\}$ is the set of customers. The set of arcs (directed edges) E is associated with a non-negative matrix $Y = (d_{ij})$, where d_{ij} represents the travel time (or equivalently the distance) of the arc $(i, j) \in E$ and the items of Y satisfy triangle inequality. Furthermore, there is a fleet H of N_v homogeneous vehicles, each with a capacity P. Each customer $i \in C$ has a demand p_i that is fulfilled when a vehicle visits the customer. A solution to the LLRP problem, after determining the opening of at most N_d depots, involves at most N_v disjoint Hamiltonian tours from these depots. Each tour starts and ends at the same opened depot, ensuring that each customer is visited exactly once by a tour. In addition, the sum of the demands of the customers in each tour must not exceed the capacity P of the vehicle of the tour. Given a feasible solution, let t_i^k be the arrival time of vehicle $k \in H$ at customer $i \in C$ ($t_i^k = 0$ if i is not served by k). Then the LLRP is to find a solution S that minimizes the sum of the waiting times of all customers.

$$Minimize \quad f(S) = \sum_{k \in H} \sum_{i \in C} t_i^k, \quad S \in \Omega \tag{1}$$

where Ω is the search space of all feasible candidate solutions for a LLRP instance. A mathematical formulation of the LLRP is provided in (Moshref-Javadi & Lee, 2016).

The LLRP was formally defined by Moshref-Javadi & Lee (2016), where two algorithms were proposed to tackle it, a memetic algorithm (MA) and a recursive granular algorithm (RGA). MA uses a solution representation consisting of two parts: the first part represents the open depots, and the second part defines the vehicle assignment and the sequence of the customers visited by each vehicle. Four different initialization methods are applied to diversify the initial population. The Order Crossover (OX) is used to generate offspring solutions, and a local search based on three move operators is applied to improve the generated offspring. In RGA, a granularity-based neighborhood search method systematically modifies the current solution, followed by a local search procedure using three move operators to further improve the solution. The authors tested the algorithm on three benchmark sets for the LRP variants, specifying the number of open depots and assigned vehicles for each instance.

Nucamendi-Guillén et al. (2022) proposed two novel mixed-integer formulations based on multi-level networks for the LLRP. Additionally, they introduced a variant of the LLRP that considers the open cost of depots. To solve the LLRP, they presented a GRASP-based iterated local search (GBILS), which includes a constructive procedure and an improvement procedure. Within each iteration of the algorithm, a feasible solution is constructed by the constructive procedure and subsequently improved by the improvement procedure. The constructive procedure randomly applies different methods to determine the opened depots. Following this, customers are selected based on their distance to the opened depots, and a given number of routes are constructed. The remaining customers are assigned to routes based on both distance and remaining vehicle capacity. In the improvement procedure, three intra-route moves are iteratively applied until the solution can no longer be improved. Then, two inter-route moves are applied to further improve the solution. Experimental results showed that GBILS was able to find several new best-known solutions.

Osorio-Mora et al. (2023b) presented three algorithms that integrate simulated annealing (SA) and variable neighborhood descent (VND) (Mladenović & Hansen, 1997) to effectively solve the LLRP. SA serves as the method to escape local optima, and the VND procedure is applied to improve the solution. Upon reaching a threshold indicating that the solution cannot be further improved, the Lin-Kernighan-Helsgaun (LKH-3) heuristic (Helsgaun, 2017) is used to improve each individual route, addressing the corresponding CCVRP. The study introduced three types of VND methods exhibiting different behaviors. Experimental results on various instances indicated that the proposed algorithm significantly outperformed the state-of-art algorithms from previous studies in the domain.

Osorio-Mora et al. (2023a) introduced an iterated local search (M-ILS) to tackle three latency vehicle routing problems with multiple depots, including

the MDCCVRP, the LLRP and the multi-depot k-traveling repairman problem. Recognizing that the proper selection of depots is critical to the success of the algorithm, the authors introduced a method that integrates LKH-3 and integer linear programming to simultaneously consider depot selection and vehicle routing. Following this, an iterative process applies a perturbation procedure, a local search based on five moves, and a SA-VND approach similar to Osorio-Mora et al. (2023b) to continually improve the quality of the solution. Then, the LKH-3 algorithm is used again to solve the CCVRP for each open depot. Experimental results showed that M-ILS stands out as the most powerful algorithm for solving the LLRP, consistently producing the best-known solutions for most benchmark instances.

These reviewed studies have continuously advanced the state of the art in solving the LLRP. However, compared to other popular routing problems, research on the problem is still limited, and additional efforts are needed to develop more powerful and robust methods capable of finding satisfactory solutions for the most challenging problem instances.

In this paper, we present a reinforcement learning guided hybrid evolutionary algorithm to address the LLRP, which includes a multi-parent edge assembly crossover and a learning-driven local search. Inspired by the edge assembly crossover for the traveling salesman problem (Nagata & Kobayashi, 2013), the proposed crossover builds offspring solutions by inheriting subtours that contribute to high-quality solutions from the parents, preserving the desired solution diversity with multiple parents, and considering edge orientation during the crossover process. The VND-based local search is reinforced by two original techniques. It uses reinforcement learning to dynamically determine the exploration order of the underlying neighborhoods. It additionally adopts strategic oscillation (Glover & Hao, 2011) to allow the VND procedure to achieve a balanced exploration between both feasible and infeasible search spaces. In terms of methodological contributions, the idea of the multi-parent edge assembly crossover can be conveniently applied to other routing problems, while the dynamic exploration of multiple neighborhoods with reinforcement learning is valuable for local search algorithms using multiple move operators.

In terms of computational contributions, we present experimental results on 76 popular benchmark instances to evaluate the performance of the algorithm. The results show that the algorithm is highly competitive with state-of-the-art algorithms, by finding 51 record-breaking results (new upper bounds) and matching all the remaining best-known results. These updated results are useful for future studies of the problem. Moreover, these results are achieved with shorter computation times than state-of-the-art methods, indicating its computational efficiency. We also perform experiments to understand the behavior of the algorithm. Finally, the codes of the algorithm will be made publicly available, which can be used by practitioners and researchers to solve related

problems.

In the remainder of the paper, we present the proposed algorithm in Section 2, a comprehensive computational comparison with leading algorithms in Section 3. Section 4 shows additional experiments to analyze the main algorithmic components and provide insights into their roles. Section 5 offers conclusions and outlines future work.

2 Reinforcement learning guided hybrid evolutionary algorithm

The proposed reinforcement learning guided hybrid evolutionary algorithm (RLHEA) for the LLRP follows the framework of the population-based memetic algorithms (MAs) (Moscato, 1999), especially MAs in discrete optimization (Hao, 2012). MAs benefit from the synergy of these two complementary search strategies and provide a powerful framework for solving difficult problems. In particular, MAs have been very successful in solving several complex routing problems (He & Hao, 2023a,b; Lu et al., 2018; Nagata, 1997; Ren et al., 2023). RLHEA is an advanced MA characterized by its multi-parent edge assembly crossover (MPEAX) and its reinforcement learning guided variable neighborhood descent with strategic oscillation (RL-SOVND). It also includes a population initialization procedure, a mutation procedure, and a population management method.

2.1 Main scheme

The general RLHEA framework is outlined in Algorithm 1. The learning functions Q and R are initialized at the beginning (line 2). The population Pop is generated by the initialization procedure (line 3). After recording the best feasible solution S_b found so far (line 4), the algorithm enters the "*while*" loop to improve the population. In each generation, three parents are randomly selected from the population (line 6). The multi-parent edge assembly crossover is then employed to generate an offspring solution (line 7). If the offspring is infeasible (i.e., violating the vehicle capacity or/and the number of opened depots), it is immediately repaired (line 9), followed by a mutation procedure to diversify the solution (line 11). Then, RL-SOVND is activated to improve the quality of the offspring (line 12). The search information is updated based on the local optimum obtained (lines 13-17), and the population is updated accordingly (line 18). During the search process, if the best solution S_b remains unchanged for a given number of consecutive generations, half of the individuals in the population are regenerated to introduce diversity (line 20). The algorithm terminates and returns the best feasible solution S_b when reaching

the predefined maximum number of generations (line 23).

Algorithm 1 Pseudo-code of RLHEA

Input: Problem instance, population size τ, population replacement threshold I_r.
Output: The best solution S_b found.

1: $I_n \leftarrow 0$ /* Counter of consecutive generations the best solution S_b is not improved */
2: $Q, R \leftarrow$ Initialize the Q-learning functions Q and R
3: $Pop = \{S_1, S_2, ..., S_\tau\} \leftarrow$ PopInitialize() /* Population initiation, section 2.2 */
4: $S_b \leftarrow arg\ min_{\forall S_i \in \text{Pop}} f(S_i)$ /* Record the best feasible solution found so far */
5: **while** *stopping condition is not reached* **do**
6: $S_A, S_B, S_C \leftarrow$RandomParentSelection(P)
7: $S \leftarrow$ MPEAX (S_A, S_B, S_C) /* Crossover, section 2.3 */
8: **if** *Is_Infeasible*(S) **then**
9: $S \leftarrow$ Repair(S) /* Repairing infeasibility, section 2.4 */
10: **end if**
11: $S \leftarrow$ Mutation(S) /* Mutation, section 2.5 */
12: $S_l, Q, R \leftarrow$ RL-SOVND(S, Q, R) /* Local improvement, section 2.6 */
13: **if** $f(S_l) < f(S_b)$ **then**
14: $S_b \leftarrow S_l, I_n \leftarrow 0$
15: **else**
16: $I_n \leftarrow I_n + 1$
17: **end if**
18: UpdatingPop(Pop, S_l) /* Population management, section 2.7 */
19: **if** $I_n > I_r$ **then**
20: ReplacingPop(Pop), $I_n \leftarrow 0$ /* Population replacement */
21: **end if**
22: **end while**
23: **return** S_b /* Return the best feasible solution found during the search */

2.2 Population initialization

The population initialization is a two-step process: depot selection and route construction, and applies a random initialization method and a greedy initialization method with an equal probability. The first step randomly selects a predefined number of depots to open. For the route construction step, note that the objective value decreases as the number of vehicles increases since the edge returning from the last customer to the depot doesn't contribute to the objective. Additionally, the weight of an edge within a route affects the waiting time of all customers following that edge. Therefore, it is important that the edge at the beginning of each route is as short as possible, while utilizing all available vehicles and maintaining a balanced distribution of customers across all routes. Building upon these considerations, the second step assigns customers to different vehicles in a cyclic manner until all customers are served. Both greedy and random methods are used to assign customers.

The greedy method first selects the shortest edge between the opened depots and the unselected customers to determine the depot and the first node until the specified number of routes is initialized. Then, each route is constructed by choosing the shortest edges between the last node of the route and the remaining unselected customers. The random method constructs the routes by selecting random depots and random customers, without using any greedy selection criterion. After a solution is constructed, it is improved using the RL-SOVND procedure, and then inserted into the population if no copy of the solution exists in the population.

2.3 Offspring generation based on MPEAX

A meaningful crossover should be able to produce promising offspring by inheriting good features from the parents (Hao, 2012). Therefore, it is important to find good features that contribute to the high-quality of solutions and to pass them on to the offspring. For the traveling salesman problem and routing problems, the common edges shared by the parents are regarded as the key feature of high-quality solutions, and this feature has enabled the design of powerful crossover operators such as the maximal preservative crossover (Mühlenbein, 1991), the partition crossover (Whitley et al., 2009; Sanches et al., 2017) and the edge assembly crossover (EAX) (Nagata, 1997; Nagata & Kobayashi, 2013). Also, EAX-like operators also performed well on the capacitated vehicle routing (Nagata, 2007) and other well-known routing problems (Nagata et al., 2010; He & Hao, 2023a,b).

For the LLRP, we introduce the multi-parent edge assembly crossover (MPEAX) that relies on the idea of the original EAX crossover for the TSP (Nagata, 1997; Nagata & Kobayashi, 2013). MPEAX also generalizes the dEAX crossover of the two-individual evolutionary algorithm (TIEA) for the MDCCVRP (Zou et al., 2024).

EAX for the TSP uses the joint graph (undirected graph) of the parent solutions to generate the so-called AB-*cycles*, where an AB-*cycle* is a cycle consisting of edges taken alternately from the parents and constitutes one core element of EAX. For the LLRP, recognizing that the direction of the route significantly impacts the objective function, we account for the route direction and use a directed graph to represent a LLRP solution. In this graph, each customer node is connected to one in-degree edge and one out-degree edge. Based on this graph representation of solutions, the proposed MPEAX crossover generalizes the notion of AB-*cycle* to the case of directed edges with three parent solutions. In addition, the presence of multiple depots in the LLRP may make it impossible to form an AB-*cycle* due to the absence of edges with the same degree related to some depots. To overcome this, we treat all depots as a sin-

gle node in our approach like in (Zou et al., 2024) for the MDCCVRP. This treatment may not result in a strict 'cycle'. So we adopt the term AB-*sequence* to accommodate this modification.

Let S_A, S_B, and S_C be three parent solutions randomly selected in the population. We define their directed graphs, $G_A = (V, E_A)$, $G_B = (V, E_B)$ and $G_C = (V, E_C)$ where $V = D \cup C$ and E_X $(X = A, B, C)$ is the set of directed edges traveled by parent solution S_X. Suppose that S_A, S_B, and S_C are recombined in this order. Then the MPEAX crossover first recombines parents S_A and S_B to get an intermediate offspring solution, which is then recombined with parent S_C to get the final offspring. The specific steps of MPEAX are described as follows and an illustrative example is provided in Fig. 1.

(1) We create a joint graph $G_{AB} = (V, (E_A \cup E_B) \setminus (E_A \cap E_B))$ from $G_A = (V, E_A)$ and $G_B = (V, E_B)$.
(2) The edges in G_{AB} are grouped into AB-*sequences*. An AB-*sequence* begins with a randomly selected node that has connected edges. Then, an adjacent edge is chosen randomly with respect to this node, and edges from G_A and G_B with the same degree for their common node are chosen to be alternately linked. When an edge connecting to the depot is selected, the next chosen edge can be any edge connected to any depot with the same degree. Once an edge is chosen such that it has the same degree as the first selected edge at the first chosen node, an AB-*sequence* is formed. This process is repeated until no edge exists in G_{AB}.
(3) The *E-set* is built by randomly selecting an AB-*sequence*, and then selecting the AB-*sequences* that share at least one node with the chosen sequence to form the *E-set*. Then take parent S_A as the base solution, remove the edges from S_A and add the edges from S_B included in *E-set*. The step leads to an intermediate solution.
(4) It is possible that the intermediate solution contains sub-tours (i.e., cycles consisting exclusively of customer nodes). If this happens, they are eliminated by the 2-opt* operator by removing two arcs (one from the sub-tour, one from the existing route) and connecting the sub-tour to the exiting route by adding two new arcs. It is also possible that some routes start and end at different depots, making the route not a cycle. To address this issue, we select the depot that is closer to the first node of the route as the depot for that route. Once this issue is solved, we obtain an intermediate offspring solution from parents S_A and S_B, we use S_O to denote this solution.
(5) The last parent solution S_C is then used to be recombined with the intermediate offspring solution S_O, following the same procedure used to crossover parents S_A and S_B. This leads to the final offspring solution.

In the example of Fig. 1, two out of the five depots (square points) are selected as the opened depots. MPEAX generates four AB-*sequences* (step 2), and AB-

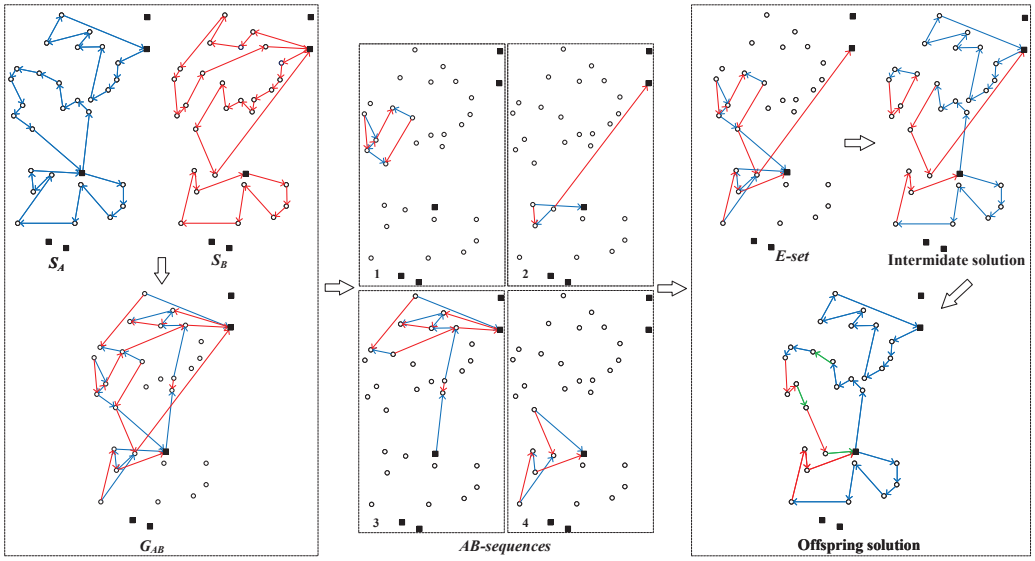

Fig. 1. Illustration of the crossover procedure.

sequence 4 is selected as the central AB-*sequence*, which shares common nodes with AB-*sequences* 1 and 2. Then the *E-set* consists of three AB-*sequences* (step 3). In the intermediate solution, there is a sub-tour (the small tour), and a tour is not a cycle (involving two depots). After fixing these problems in step 4, three new arcs are introduced, shown in green, leading to the final offspring.

2.4 Repair procedure

MPEAX can generate infeasible offspring with more open depots than allowed. In addition, since MPEAX does not take vehicle capacity into account, the capacity constraint may be violated. To address these issues, we use a two-step procedure to repair an infeasible offspring solution. The first step ensures that the number of open depots doesn't exceed the allowed limit, while the second step focuses on repairing capacity violations.

If the number of open depots exceeds the given limit N_d, we use two repair methods. The first method relies on the frequency information of each depot being selected in the high-quality solutions returned by the local search procedure (RL-SOVND). Among the open depots, the top N_d depots with the highest frequency in the offspring being repaired are retained. The second method randomly selects N_d depots. Once the open depots are determined, the routes involved in the discarded depots are reassigned using a greedy approach. Each such route is assigned to an open depot such that it is the closest depot to the first node of that route.

To deal with capacity violations, we use the inter-neighborhood operator 2-opt* to reassign customer nodes. we assess a solution using the modified objective function F of Section 2.6.3, with the penalty parameter β set sufficiently large to strongly penalize capacity violations. The procedure terminates when a feasible solution is reached or when all neighborhood solutions induced by 2-opt* have been explored. Note that this repair procedure doesn't guarantee the feasibility of capacity. The purpose of the capacity repair is to bring the input solution as close to the feasible space as possible. The RL-SOVND procedure that follows will take care of the infeasibility issue because it examines both feasible and infeasible solutions.

2.5 Mutation

After the MPEAX procedure, which is designed to preserve shared edges of the parents that contribute to high quality solutions, there may be a high degree of similarity between the offspring and the parents. To ensure a diversified offspring solution, a mutation is applied, with a probability m_p, to modify the offspring with two operators: the depot swap for the depots and the ejection chain for the customers. The depot swap operator selects a depot randomly from the set of unopened depots and uses it to replace a randomly selected open depot. The ejection chain operator randomly selects three customer nodes from different routes and swaps their positions in a cyclic manner. This mutation operation is performed m_l times (m_l is called the mutation length). After the mutation procedure, new edges not present in the parent solutions are introduced, and different depot configurations are explored.

2.6 Reinforcement learning guided VND with strategic oscillation

Our local search method, which is another critical component in our MA algorithm, is a reinforcement learning guided variable neighborhood descent with strategic oscillation (RL-SOVND). RL-SOVND is characterized by two original features. It explores multiple neighborhoods according to a dynamic order determined by reinforcement learning. To examine candidate solutions, it uses strategic oscillation to consider both feasible and infeasible solutions in a carefully controlled manner.

2.6.1 Rationale and general RL-SOVND framework

RL-SOVND explores multiple neighborhoods sequentially with the VND framework (Mladenović & Hansen, 1997), raising the important question of how to

determine the order of checking these neighborhoods. Two common strategies for determining this order are the random strategy and the prefixed-order strategy. The random strategy inspects the given neighborhoods in a random order. The prefixed-order approach examines the neighborhoods in a fixed sequence, typically determined according to the computational complexity of the neighborhoods.

However, the random approach does not differentiate the neighborhood structures and ignores the intrinsic differences between the neighborhoods. On the other hand, when using the predefined approach, one faces the difficulty of determining an appropriate order for neighborhood inspection. In addition, the best order may change during the search process, making it impossible to find an all-time best order. An interesting alternative strategy for neighborhood examination is to determine the order according to the specific problem instance to be solved and the search context of the algorithm.

To do this, we consider the determination of the neighborhood exploration order as a sequential decision-making problem and use reinforcement learning to dynamically make the best possible decision. In particular, RL-SOVND uses the renowned reinforcement learning algorithm Q-learning (Watkins & Dayan, 1992).

On the other hand, it is known that visiting infeasible solutions during the search process can be beneficial, as shown in studies on constrained problems (Li et al., 2024; Wei et al., 2023; Zhou et al., 2021). This benefit arises from the increased freedom it provides to visit infeasible solutions, allowing the algorithm to more effectively transition between different feasible search regions via infeasible regions. In RL-SOVND, we use the general strategic oscillation method (Glover & Hao, 2011), which allows the algorithm to search in both feasible and infeasible regions with a focus on feasible and infeasible boundaries. For this, we devise a mechanism to prevent, based on a penalty parameter β and search information, the algorithm from getting stuck in either feasible or infeasible space for too long.

Algorithm 2 shows the general RL-SOVND framework. Initially, the penalty parameter β (Section 2.6.3) is set based on the objective value $f(S)$ of the input solution S and the total customer demand $\sum_{i \in C} p_i$ (line 3). The algorithm then enters the main loop to improve the current solution (lines 5-29). Within this loop, the neighborhood structures included in the set N (see Section 2.6.3) are systematically explored. The selection of the next neighborhood N_δ to be examined is determined using Q-learning (line 10, Section 2.6.2). This is done based on the current state St (comprising the explored neighborhood structures) and the historical search information contained in the Q-table Q and the reward matrix R. For the chosen neighborhood N_δ, the neighborhood solutions are explored using the first improvement strategy (line 11). Subse-

Algorithm 2 Pseudo-code of RL-SOVND

Input: Input solution S, set of neighborhoods N, slide window length u_p, Q-table Q, reward matrix R
Output: Local optimum S_l, updated Q-table Q, and reward matrix R

1: $I_f, I_i \leftarrow 0$ /* Set counters on consecutive feasible and infeasible solutions */
2: $Improve \leftarrow$ true
3: $\beta \leftarrow \frac{f(S)}{\sum_{i \in C} p_i}$ /* Initialize the penalty parameter β */
4: $S_l \leftarrow S$ /* Record the local optimum solution */
5: **while** $Improve$ **do**
6: $Improve \leftarrow$ false
7: $n_e \leftarrow 0$ /* Initialize the number of explored neighborhood structures */
8: St.clear() /* Set the current state of explored neighborhoods */
9: **while** $n_e < |N|$ **do**
10: $N_\delta \leftarrow$ Q-learning(St, Q, R)
11: $S' \leftarrow S \oplus N_\delta$ /* Perform the first improvement with N_δ */
12: St.append(N_δ) /* Update the state */
13: Update Q, R /* See Section 2.6.2 */
14: **if** $F(S') < F(S)$ **then**
15: $S \leftarrow S'$ /* Accept a better solution under F, see Section 2.6.3 */
16: **if** $Is\_feasible(S')$ and $f(S') < f(S_l)$ **then**
17: $S_l \leftarrow S'$ /* Update the local optimum solution */
18: **end if**
19: Update I_i, I_f
20: **if** $I_i > u_p$ or $I_f > u_p$ **then**
21: Adjust the penalty parameter β /* See Section 2.6.3 */
22: **end if**
23: $Improve \leftarrow$ true
24: **break**
25: **else**
26: $n_e \leftarrow n_e + 1$
27: **end if**
28: **end while**
29: **end while**
30: **return** S_l, Q, R /* Return S_l, Q, and R */

quently, St, Q and R are updated based on the outcome of the executed action (lines 12-13). If an improved solution S' is found in the neighborhood N_δ under the extended objective function F (Section 2.6.3), the current solution S is updated (line 15). Moreover if S' is feasible and is better than the recorded best feasible solution found during the current RL-SOVND run, S_l is also updated by S' (line 17). The counter for consecutive accepted feasible or infeasible solutions is also updated (line 19), and the penalty parameter β is adjusted if the predefined condition is met (lines 20-21). Then, the algorithm returns to the beginning of the main loop (line 23). If no improvement is achieved with the current neighborhood, the next neighborhood structure is explored. The algorithm terminates after exploring all neighborhood structures without

improvement, and the best local optimum solution S_l, the updated Q-table Q and reward matrix R are returned (line 30).

2.6.2 Q-learning for deciding the exploring order

Q-learning uses the so-called Q-value function to estimate the expected long-term cumulative reward associated with performing a particular action within a given state. We use Q-learning to determine the most suitable neighborhood to explore in order to improve the current solution, considering that some neighborhoods have already been explored. We define the fundamental notations of Q-learning including states, actions, transition policy, and rewards used in our algorithm as follows.

- States (ST): The state set comprises the explored neighborhood structures.
- Actions (A): The set of available actions depends on the current state. In a given state st, there is a specific action set denoted as $A(st)$, consisting of the neighborhood structures that have not yet been examined.
- Rewards (R): An immediate reward $r = R(st, a)$ is assigned when an action $a \in A(st)$ is executed at the current state st. The reward matrix R is updated after the selected neighborhood is examined. Further details about the updating process can be found below.
- Transition policy: The algorithm employs an ε-greedy policy to govern state transitions between different states. This policy selects with a probability of ε the action a^* from the action set $A(st)$ of current state st that maximizes the Q-value, i.e., $a^* = \arg\max Q(st, a)$, where $a \in A(st)$. Meanwhile, there is a probability of 1-ε to randomly choose an action.

After the execution of the chosen action, the Q-table is updated according to Equation 2.

$$Q(st, a) = (1 - \alpha)Q(st, a) + \alpha[R(st, a) + \gamma \max_{a' \in A(st')}(Q(st', a'))] \tag{2}$$

In this equation, st represents the current state, a corresponds to the current action, st' denotes the next state resulting from the current action a, and α and γ, both in the range of [0,1], are the learning rate and discount factor, respectively. The values stored in R represent the reward values associated with specific actions in a given state. When an action is executed, either an improved solution or a local optimal solution among all the neighbourhood solutions is found, denoted as S_r. We use the objective value $f(S_r)$ of S_r to update the reward value associated with the state-action pair. We define two terms: $\Delta_r = f(S_c) - f(S_r)$, which can be either positive or negative, and $\Delta_b = f(S_b) - f(S_r)$, where S_c represents the current solution before executing

the selected neighborhood, and S_b is the global best solution found. The update mechanism for the reward values is described by Equation 3.

$$R(st,a) = \begin{cases} \xi R(st,a) + \Delta_r + max(0,\Delta_b)e^{|N|-|A(st)|} & \text{if } \Delta_r > 0 \\ \xi R(st,a) + \Delta_r & \text{if } \Delta_r < 0 \end{cases} \tag{3}$$

where ξ denotes the discount coefficient, set to 0.95. This coefficient is used to reduce the influence of historical information and to give more weight to recent performance. N is the set of neighborhoods (see Section 2.6.3). In particular, when a new best solution is found, an additional bonus reward is given, which increases with the number of neighborhoods explored. This is because more reward should be given as high-quality neighborhood solutions become scarcer.

2.6.3 Variable neighborhood descent with strategic oscillation

The VND procedure in our algorithm explores seven distinct neighborhood structures induced by the following move operators.

N_1 (*Relocate*). It relocates a customer node from its initial location to another position within the same or a different route.

N_2 (*Swap*). It is associated with both customer nodes and depot nodes. It involves swapping the positions of two nodes, which can be from the same or different routes. The nodes to be swapped must be of the same type, i.e. a customer node can only be swapped with another customer node, and similarly for depot nodes.

N_3 (2-*opt*). It can be applied to the nodes within the same route (intra-route) or the nodes of different routes (inter-route). The intra-route operator deletes two non-adjacent edges and adds two new edges. Meanwhile, the edges between the deleted edges are reversed. The inter-route operator, also called *2-opt**, deletes two edges and adds two new edges.

N_4 (2-*relocate*). It relocates two consecutive customer nodes from their original positions to different locations within the same or different routes.

N_5 (*Node-arc swap*). It swaps the positions of a customer node and an arc (two consecutive customer nodes), which can occur within the same route or between different routes.

N_6 (*Arc-arc swap*). It swaps two consecutive customer nodes from either the same or different routes.

N_7 ($Swap*$). This is an inter-route operator that selects two customers from different routes, removes them from their original positions, and inserts them into the best position within each other's route. This move operator is only executed when the routes of the selected customers overlap, following the approach in Vidal (2022).

It's worth noting that we limit the neighborhood of each customer to include only the δ-nearest vertices, where $\delta < |V|$. The reason for this is that solutions involving edges with long distances are less likely to be of high quality. This method increases the computational efficiency by avoiding the examination of less promising solutions. Notably, this approach has been shown to be effective in solving other routing problems (Helsgaun, 2000; Toth & Vigo, 2003).

RL-SOVND uses the general strategic oscillation method (Glover & Hao, 2011) to explore both feasible and infeasible solutions within these neighborhood structures. To evaluate an infeasible solution, we define an extended objective function F, as shown in Equation 4, which is a combination of the objective function f and a penalty term to deal with constraint violations, where r_k is the set of customers visited by vehicle k. The second term in this equation represents the degree to which the vehicle capacity is exceeded by the vehicles used. The penalty parameter β is used to balance the exploration of feasible and infeasible search spaces and is dynamically adjusted using search information. This helps the algorithm not to get stuck in feasible or infeasible space for too long.

$$F(x) = f(x) + \beta \sum_{k \in H} max(0, \sum_{i \in r_k} p_i - P) \tag{4}$$

Specifically, the VND procedure maintains a sliding window of length of u_p iterations to evaluate the feasibility of the accepted solutions within the window. If all accepted solutions are feasible, we decrease the penalty parameter to promote exploration of infeasible spaces. Conversely, if all solutions in the window are infeasible, we increase the penalty parameter to encourage the algorithm to explore feasible spaces. If both feasible and infeasible solutions are accepted within the window, we keep the penalty parameter unchanged. The specific method for adjusting this parameter is shown in Equation 5 where I_i is the number of accepted infeasible solutions in the sliding window, I_f is the number of accepted feasible solutions, u_p is the predefined threshold for adjusting β, and $rand(0, 1)$ is a random number 0 or 1.

$$\beta = \begin{cases} \beta(1.5 + rand(0,1)) & \text{if } I_i = u_p \\ \frac{\beta}{1.5+rand(0,1)} & \text{if } I_f = u_p \end{cases} \quad (5)$$

2.7 Population updating

Population updating aims at maintaining an appropriate diversity among the solutions in the population. The updating mechanism used takes into account both the quality of the solution and its contribution to the population diversity. The contribution to diversity is assessed by measuring the distance between the new solution and the population.

Given two solutions, S_a and S_b, their distance is the number of non-common edges between the solutions, which is determined by Equation 6, where E represents the arc set of a solution. Accordingly, the distance between a solution and the population is defined as the minimum distance between this solution and any solution from the population (excluding itself if it is also part of the population), as shown in Equation 7.

$$IDist(S_a, S_b) = |E_a| - |E_a \cap E_b| \quad (6)$$

$$PDist(S, Pop) = min\{IDist(S, S_i) : S_i \in Pop \setminus S\} \quad (7)$$

We employ this method to determine whether a new solution from the local search procedure (RL-SOVND) should be added to the population. We first check if there is a clone of the new solution in the population (i.e., $PDist(S, Pop) = 0$). If this is the case, we discard the new solution. Otherwise, we add the new solution into the population, resulting in a modified population called Pop'. Next, we re-evaluate the fitness of all solutions in Pop' using their quality and distance to this population by Equation 8, and the solution with the worst fitness value is removed from the population. In this equation, a normalization is applied since the quality and distance values are not of the same dimension. We define $f_{max} = \max\{f(S_i) : S_i \in Pop'\}$ and $f_{min} = \min\{f(S_i) : S_i \in Pop'\}$ as the maximum and minimum objective values within the population Pop'. Additionally, $PD_{max} = \max\{PDist(S_i, Pop') : S_i \in Pop'\}$ and $PD_{min} = \min\{PDist(S_i, Pop') : S_i \in Pop'\}$ represent the maximum and minimum distances between the solutions and the population. The parameter ψ is empirically set to 0.55.

$$fit(S) = \psi \frac{f_{max} - f(S)}{f_{max} - f_{min}} + (1 - \psi) \frac{PDist(S, P') - PD_{min}}{PD_{max} - PD_{min}} \tag{8}$$

If the best solution found so far is not updated during I_r (set to 1000) consecutive generations, indicating a search stagnation, we introduce diversity into the population to facilitate escape from deep local optima. First, we randomly remove half of the solutions in the population, while keeping the best solution. Then, for the given population size, new solutions are added either using the random initialization method (Section 2.2) or by randomly selecting solutions from an adaptive memory M. The adaptive memory stores the most recent 3000 local optima found by the local search procedure RL-SOVND. To introduce more diversity into the population, only solutions in the first half of M are considered, corresponding to the solutions added to the memory earlier.

2.8 Discussions

Our RLHEA algorithms has a number of novelties compared to the existing methods.

The MPEAX crossover is derived from the dEAX crossover of the two-individual evolutionary algorithm (TIEA) for the CCVRP and MDCCVRP (Zou et al., 2024), which can be regarded as special cases of the LLRP. MPEAX is divided into two phases, each with two parent solutions. For each phase, MPEAX and dEAX share the same operations for the first three steps, while the remaining two steps are different. In fact, since the number of open depots in the LLRP is limited, the intermediate solution (step 4) may require solution repair by selecting the given number of open depots.

In addition, MPEAX extends the dEAX crossover by incorporating three parent solutions to mitigate the loss of diversity resulting from considering the direction of edges during the crossover procedure. When using three parent solutions, the crossover order of the three parents needs to be carefully considered. Indeed, compared to the first two parents, the features of the last parent are only diluted once by crossover, increasing the opportunity of transmitting its edges to the offspring solution. For MPEAX, based on this observation, we select the individual with the shortest life in the population (inserted into the population last) as the third parent, which effectively enhances the diversity of the population.

Compared to the work (Moshref-Javadi & Lee, 2016), which uses a simple OX crossover applied to a giant tour, the MPEAX crossover allows the offspring

to naturally inherit the common edges from the parents. This is beneficial for creating more promising offspring and thus increasing the search efficiency of the algorithm.

Finally, our local search procedure, RL-SOVND, follows the general VND framework, which relies on multiple neighborhoods. This raises the critical issue of determining the best exploration order of the adopted neighborhoods. Compared to other methods that also use VND to solve routing problems (Ren et al., 2023; Zou et al., 2024), our RLHEA algorithm differs in its approach to learn the best neighborhood exploration order from the search information. In fact, most existing methods explore their neighborhoods in a fixed or random order. In contrast, RLHEA uses Q-learning to dynamically determine the best neighborhood exploration order. This adaptive approach makes RLHEA more effective and improves its performance, as demonstrated in Section 4.3. And it can be applied to any local search algorithm involving a portfolio of neighborhoods or search operators.

3 Computational results

We now present an extensive computational evaluation of the RLHEA algorithm on the benchmark instances for the LLRP and a comparison with the state-of-the-art algorithms.

3.1 Benchmark instances

We use three sets of 76 benchmark instances introduced by Moshref-Javadi & Lee (2016).

Set Tuzun-Burke: This dataset consists of 36 instances with 100 to 200 customers and 10 to 20 depots, and is considered as the most challenging of the benchmark instances. No optimal solutions have been reported in this set.

Set Prodhon: This dataset contains 30 instances with 20 to 200 customers and 5 to 10 depots. 11 instances have been solved optimally in the literature.

Set Barreto: This dataset consists of 10 instances with 21 to 134 customers and 5 to 14 depots. Six instances with less than 50 customers have been solved optimally in the literature.

The RLHEA algorithm has the following main parameters: mutation probability m_p, mutation length m_l, learning rate α, discount factor γ, greedy probability ε, length of the sliding window u_p, and neighborhood reduction parameter δ. To determine suitable values for these parameters, we employed the automatic parameter tuning package Irace (López-Ibáñez et al., 2016). Through the tuning process, we obtained the configuration presented in Table 1. This configuration represents the default parameter setting for our algorithm. Moreover, RLHEA uses a population of 20 individuals.

Table 1
Parameter tuning results

Parameter	Related section	Description	Considered values	Final values
m_p	2.5	mutation probability	{0,0.1,0.2,0.3}	0.1
m_l	2.5	mutation length	{1,2,3,4,5}	2
α	2.6.2	learning rate	{0.1,0.2,0.3,0.4,0.5}	0.2
γ	2.6.2	discount factor	{0.8,0.85,0.9,0.95}	0.85
ε	2.6.2	probability of ε-greedy	{0.7,0.75,0.8,0.85,0.9,0.95}	0.7
u_p	2.6.3	length of the slide window	{2,4,6,8,10}	4
δ	2.6.3	granularity threshold	{10,15,20,25,30}	20

According to the literature review in Section 1, four studies have addressed the LLRP problem. The earliest algorithm MA (Moshref-Javadi & Lee, 2016) retains only few best-known solutions. Consequently, we have excluded it from our comparative study. The reference algorithms for comparison include GBILS proposed in (Nucamendi-Guillén et al., 2022), three algorithms (SA-VND0, SA-VND1, SA-AND2) introduced in (Osorio-Mora et al., 2023b), and the M-ILS algorithm presented in (Osorio-Mora et al., 2023a). The M-ILS algorithm has two versions, one yielding superior results with 30 runs and another with 5 runs; in our study, we exclusively compared with the former (with 30 runs). For the *Set Tuzun-Burke*, there is no result reported for the GBILS algorithm. Among these algorithms, M-ILS stands out as the most powerful, retaining almost all of the current best-known solutions.

Our RLHEA algorithm was programmed in C++ and compiled using the g++ 10.2.1 compiler with the -O3 optimization option. The experiments were conducted on a Xeon E5-2670 processor operating at 2.5GHz with 2GB RAM, running Linux with a single thread. Our algorithm was executed 30 times for each instance, following the approach employed by M-ILS. The stopping condition for our algorithm was set to 5000 generations (crossovers). For the three algorithms SA-VND0, SA-VND1, SA-VND2, and the M-ILS algorithm, the authors generously provided the C++ source codes that we ran on our computer, making it possible to perform a fair comparative study. The algorithm parameters and stopping conditions are set to match the criteria outlined in the original paper. The tested instances and the best solutions achieved by

our algorithm are accessible online [1], and the code of our RLHEA algorithm will also be made publicly available.

3.3 Computational results and comparison

Table 2 provides a summary of the comparative results on the three datasets between our RLHEA algorithm and the reference algorithms, while Tables A.1–A.3 of the Appendix show the detailed results, including the best and average objective values as well as the average CPU running time. In Table 2, the first column represents the dataset. Columns f_{best} and f_{avg} provide a summary in terms of the best and average objective values achieved among 30 independent runs. The column labeled "#Wins" indicates the number of instances where RLHEA outperformed the reference algorithm, "#Ties" shows the number of instances with equal results, and "#Losses" indicates the number of instances where RLHEA performed worse than the reference algorithm. The p-values from the Wilcoxon signed-rank test (with a significance level of 0.05) applied to the best and average values are also indicated, verifying the statistical significance of the performance differences between RLHEA and each reference algorithm. "BKS" represents the best-known solutions ever reported so far in the literature.

The results in Table 2 show that our RLHEA algorithm is highly competitive compared to the reference algorithms in the best and average objective values. Overall, RLHEA achieved new best-known solutions for 51 (out of 76) instances and matched all best-known results for the remaining instances (with no worse results). Specifically, for the most challenging set *Tuzun-Burke*, our algorithm discovered 31 new record-breaking solutions out of the 36 instances. For the set *Prodhon*, RLHEA reported 18 new best results out of the 19 instances whose optimal solutions were unknown, and for the set *Barreto*, it reached new best results for 2 out of the 4 instances with unknown optimal solutions. Regarding the average objective value, RLHEA outperforms the reference algorithms in all instances in the set *Tuzun-Burke*. For the set *Prodhon* and the set *Barreto*, RLHEA also reports many better average results with no worse results. The p-values for f_{best} and f_{avg}, excluding the set *Barreto* due to the small sizes of the instances, are all less than 0.05.

3.4 Assessment of computational efficiency

From the detailed results of Tables A.1–A.3, we observe that our algorithm exhibits significant competitiveness in running time compared to the leading

[1] https://github.com/YujiZou/LLRP

Table 2
Summarized comparison results of RLHEA against the reference algorithms in terms of the best and average objective values on the three sets of 76 LLRP instances.

Instance	Pair algorithms	f_{best}				f_{avg}			
		#Wins	#Ties	#Losses	p-value	#Wins	#Ties	#Losses	p-value
Tuzun-Burke	RLHEA vs. BKS	31	5	0	1.32e-5	-	-	-	-
	RLHEA vs. MILS	32	4	0	9.0e-6	36	0	0	2.84e-6
	RLHEA vs. SA-VND0	36	0	0	2.84e-6	36	0	0	1.53e-6
	RLHEA vs. SA-VND1	35	1	0	3.56e-6	36	0	0	1.41e-6
	RLHEA vs. SA-VND2	35	1	0	3.86e-6	36	0	0	1.53e-6
Prodhon	RLHEA vs. BKS	18	12	0	1.96e-4	-	-	-	-
	RLHEA vs. MILS	19	11	0	1.32e-4	27	3	0	5.61e-6
	RLHEA vs. SA-VND0	21	9	0	5.96e-5	26	4	0	8.29e-6
	RLHEA vs. SA-VND1	21	9	0	5.96e-5	26	4	0	8.30e-6
	RLHEA vs. SA-VND2	21	9	0	5.96e-5	26	4	0	8.30e-6
	RLHEA vs. GBILS	26	4	0	8.30e-6	-	-	-	-
Barreto	RLHEA vs. BKS	2	8	0	0.18	-	-	-	-
	RLHEA vs. MILS	3	7	0	0.11	8	2	0	0.01
	RLHEA vs. SA-VND0	3	7	0	0.11	7	3	0	0.02
	RLHEA vs. SA-VND1	4	6	0	0.07	7	3	0	0.02
	RLHEA vs. SA-VND2	4	6	0	0.07	6	4	0	0.03
	RLHEA vs. GBILS	3	5	0	0.11	-	-	-	-

algorithms SA-VND0, SA-VND1, SA-VND2, and M-ILS. To further demonstrate the effectiveness of our algorithm, we conducted a Time-to-Target analysis (TTT) (Aiex et al., 2007). This analysis measures the time required for each algorithm to achieve a solution with an objective value at least as good as a predefined target objective value. The TTT presents the empirical probability distributions within the given time to reach the target value. In our TTT analysis, we performed each algorithm (with the source code) 100 times on different instances, recording the time taken to reach the target value. Subsequently, we sorted the times in ascending order and calculated the probability $\rho_i = (i - 0.5)/100$ for each time T_i, where T_i represents the ith smallest time.

Fig. 2 illustrates the TTT plots for four large instances (122122, 123112, 123212, 200-10-1b) from the set *Tuzun-Burke* and set *Prodhon*. The x-axis represents the time needed to reach the target value, while the y-axis represents the cumulative probability ρ_i of reaching the given target value. The figures show that the TTT curves of our algorithm are consistently above the curves of the reference algorithms, indicating that our algorithm always has a higher probability of reaching the given target value within the same running time. This experiment shows the competitiveness of RLHEA with state-of-the-art algorithms in terms of computational and search efficiency.

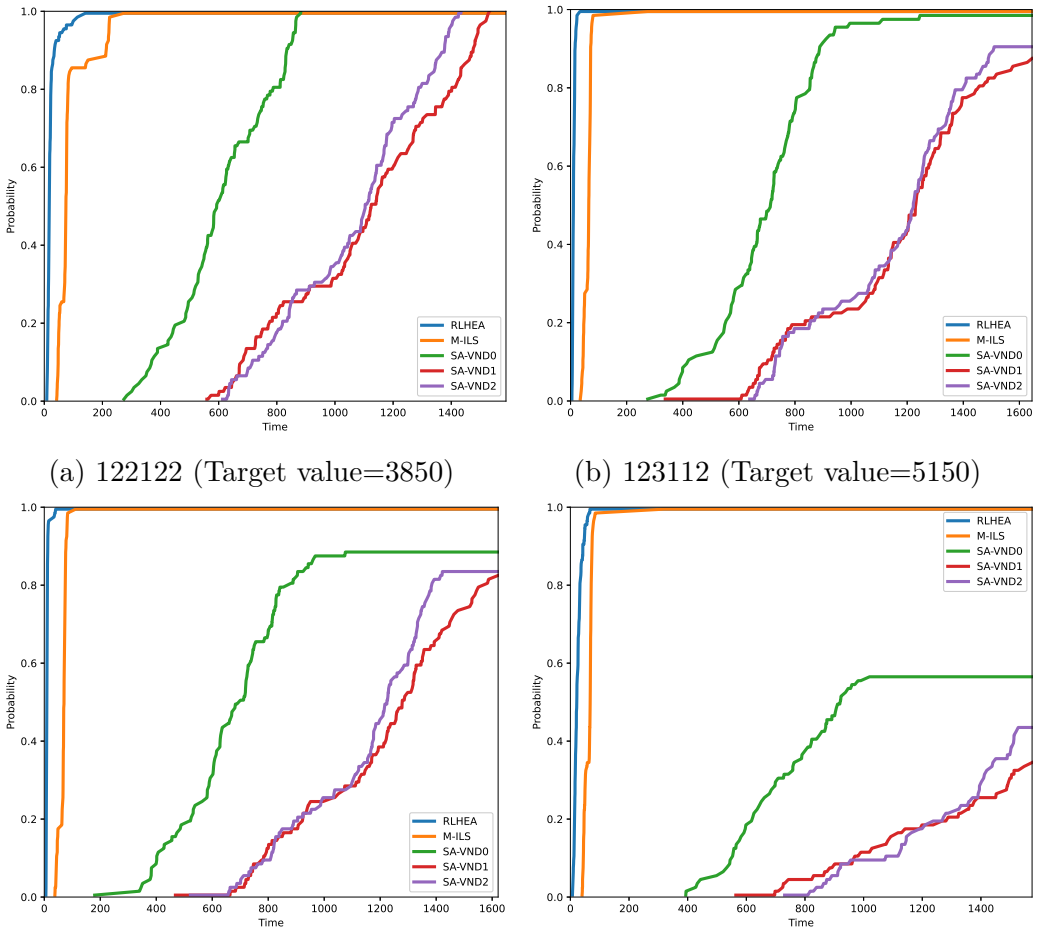

(a) 122122 (Target value=3850)

(b) 123112 (Target value=5150)

(c) 123212 (Target value=5300)

(d) 200-10-1b (Target value=3500)

Fig. 2. Cumulative probability distribution for the time to reach a target value.

4 Analysis

In this section, we conduct additional experiments to gain deeper insights into the individual influences of the main components of the RLHEA algorithm. We focus on the critical components: the MPEAX crossover, the Q-learning method and the strategic oscillation method.

4.1 Rationale behind the MPEAX crossover

Previous studies on the TSP (Nagata & Kobayashi, 2013), the VRP (Arnold & Sörensen, 2019), and their variants (He & Hao, 2023a) have revealed that high-quality solutions in these problems often share many common edges, which are likely to be part of the optimal solution. We show experimentally that this is also true for the LLRP, which provides a basis for the MPEAX crossover. Indeed, like the EAX crossover for the TSP, the MPEAX crossover

takes advantage of this property by transferring common edges from parent solutions to the offspring, while introducing new edges to increase the diversity of the offspring.

For this study, we focus on two representative instances 121222 and 200-3-1. We ran RLHEA to solve each instance 50 times and collected 15 distinct high-quality local optimal solutions in each run, resulting in a total of 750 unique local optimal solutions per instance. We sorted these 750 solutions in increasing order of their objective values and selected the top 250 (best) solutions and the 250 worst solutions to form the final set of 500 solutions. We then calculated the number of common arcs for each pair of solutions and presented the results as a heat map, as shown in Fig. 3(a) and Fig. 4(a). The x-axis and y-axis represent the rank of the solutions in the solution set, and the color represents the number of common arcs. A color closer to red indicates more common arcs, while a color closer to blue indicates fewer common arcs. To further illustrate this property, in Fig. 3(b) and Fig. 4(b) we show the percentage of arcs that a solution S shares with the best solution, where the percentage is calculated by $\frac{|E_b \cap E_s|}{|E_s|}$, where E_b is the arc set of the best solution and E_s is the arc set of the solution S.

The heatmaps of the two studied instances exhibit the same trend, we can clearly see that the lower-left corner, where the shared edges between high-quality solution pairs are shown, is colored with deep red. The top-right is colored with blue, indicating that solution pairs with poor objective values share fewer edges. Additionally, in the figures showing the relationship between the objective value and the number of shared edges with the best solution, we observe the trend that solutions with higher objective values share more edges with the best solution.

We can conclude that in the LLRP, high-quality solutions also share a high number of common edges, which provides a foundation for the MPEAX crossover to inherit common edges from the parents during the crossover process.

4.2 Benefits of the MPEAX crossover

As presented in Section 2.3, RLHEA's MPEAX crossover uses three parent solutions to address the problem of diversity degradation due to edge orientation considerations in the crossover process. To study the benefits of this method, we created two algorithm variants, RLHEA1 and RLHEA2. In RLHEA1, we replaced MPEAX with the order crossover used in Moshref-Javadi & Lee (2016) for the LLRP. In RLHEA2, we applied the MPEAX crossover to only two parent solutions. The remaining components for the two algorithm variants are identical to RLHEA, including the stopping condition set

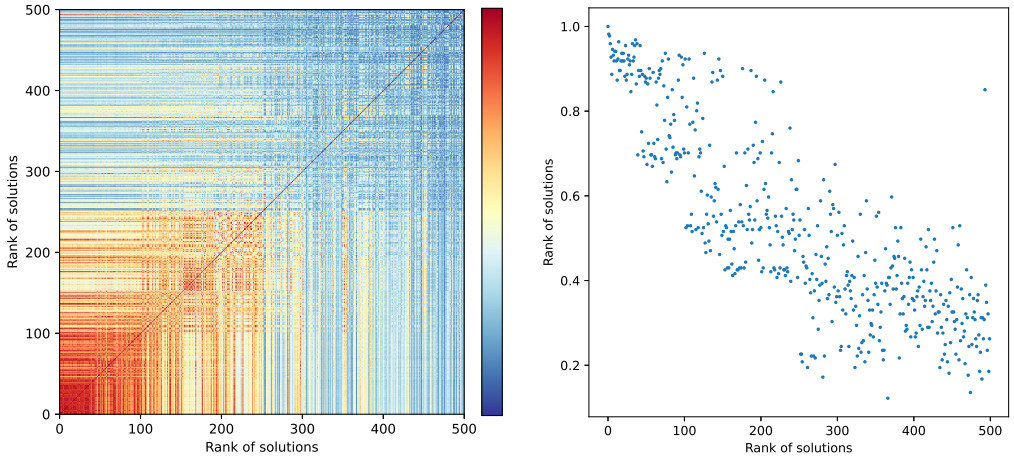

(a) Solution pair shared arc heatmap (b) Arc sharing ratio plot

Fig. 3. The heatmap for the number of shared edges of solution pairs and the scatter plot for edge sharing ratio between solutions and the best-known solution on instance 121222.

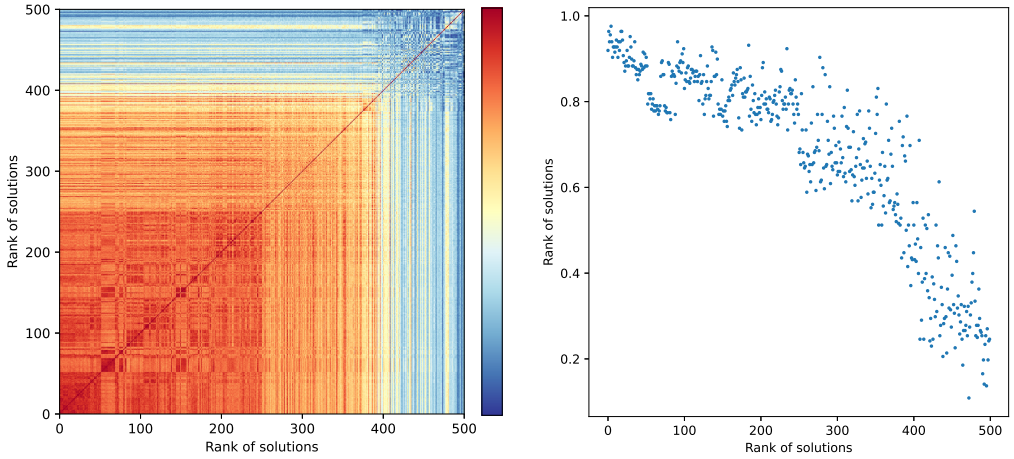

(a) Solution pair shared arc heatmap (b) Arc sharing ratio plot

Fig. 4. The heatmap for the number of shared edges of solution pairs and the scatter plot for arc sharing ratio between solutions and the best-known solution on instance 200-3-1.

to 5000 generations. We ran the algorithm variants on the large instances with at least 100 customers from the sets *Tuzun-Burke* (36 instances) and *Prodhon* (18 instances).

Table 3 shows the comparative results of RLHEA with the two variants in terms of the best and average objective values over 30 independent runs, along with the p-values from the Wilcoxon signed-rank test. Fig. 5 shows the deviation of the two variants from the reference values given by RLHEA. In Fig. 6, we present violin plots of the three algorithms on four large instances (121122, 121212, 123122, and 200-10-2), illustrating the distribution of objective values

for the solutions obtained over the 30 independent runs. Looking at the results, it is evident that the RLHEA algorithm with the three-parent MPEAX crossover significantly outperforms the two variants, especially in terms of the average values, confirmed by the small p-values. The violin plots clearly show that the solutions found by our RLHEA are more stable, demonstrating its robustness compared to the two variants. We conclude that RLHEA benefits from the edge assembly crossover method and the use of multiple parents in the crossover procedure.

Table 3
Summarized comparison results of RLHEA against the RLHEA1 and RLHEA2 variants in terms of the best and average objective values on the 54 large instances.

Instance	Pair algorithms	f_{best}				f_{avg}			
		#Wins	#Ties	#Losses	p-value	#Wins	#Ties	#Losses	p-value
Tuzun-Burke (36)	RLHEA vs. RLHEA1	12	24	0	2.22e-3	33	1	2	2.77e-2
	RLHEA vs. RLHEA2	6	30	0	4.95e-6	27	6	3	7.68e-6
Prodhon (18)	RLHEA vs. RLHEA1	7	11	0	1.80e-2	16	1	1	6.00e-4
	RLHEA vs. RLHEA2	2	16	0	0.18	15	2	1	9.35e-4

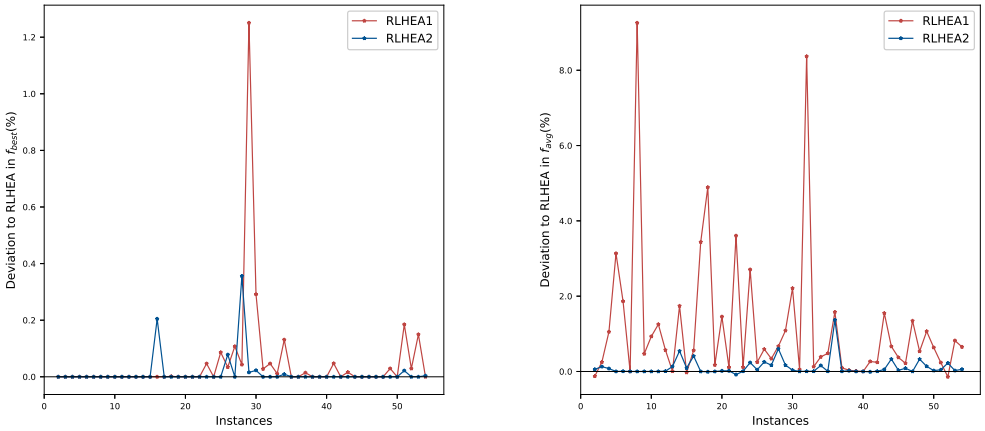

(a) Best objective value (b) Average objective value

Fig. 5. Comparative results of RLHEA with its two variants RLHEA1 and RLHEA2 on the 54 large instances.

4.3 Benefits of Q-learning

As shown in Section 2.6.3, the local search procedure uses Q-learning to determine the order in which the seven neighborhoods are explored. To evaluate the usefulness of this method, we created two algorithm variants, RLHEA3 and RLHEA4. The only difference between the two variants is the order of neighborhood exploration during local search, while the rest of the procedures remains the same. RLHEA3 uses a random order for neighborhood exploration,

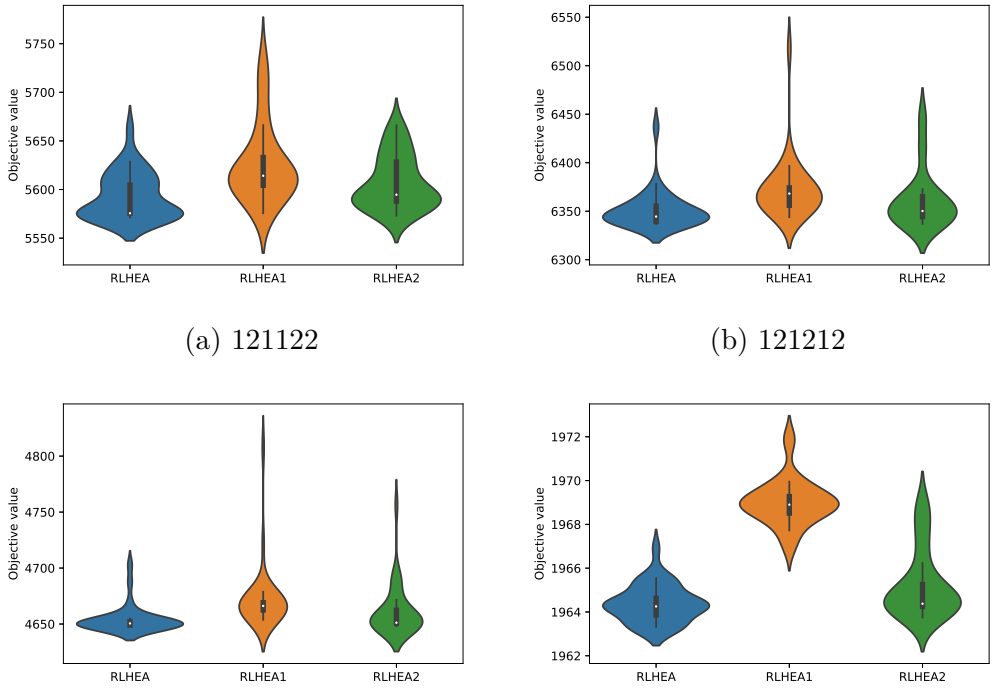

(a) 121122 (b) 121212

(c) 123122 (d) 200-10-2

Fig. 6. Violin plots of RLHEA, RLHEA1 and RLHEA2 for four instances.

while RLHEA4 explores the neighborhoods in the fixed order N_1-N_2-N_3-N_4-N_5-N_6-N_7, which reflects the increasing complexity of these neighborhoods. We ran both algorithms on the 54 large instances as in Section 4.2.

Table 4 summarizes the comparison of the results of RLHEA, RLHEA3 and RLHEA4 in terms of the best and the average objective values. Additionally, Fig. 8 shows violin plots for the three algorithms on four instances (121122, 121212, 123122, and 200-10-2), indicating the deviation of the two variants from the reference values of RLHEA. The results show that RLHEA outperforms RLHEA3 and RLHEA4 in terms of the best objective values and especially in terms of the average objective values. The violin plots further show that the solution distribution obtained by RLHEA is more stable. In conclusion, the RLHEA algorithm performs better than the variants, benefiting from the Q-learning method to determine the exploration order of neighborhoods.

4.4 Benefits of strategic oscillation

As shown in Section 2.6, RLHEA uses strategic oscillation to examine both feasible and infeasible solutions by adaptively adjusting the penalty parameter β. To evaluate the benefit of this method, we created two variants, RLHEA5 and RLHEA6. RLHEA5 visits only feasible solutions, while RLHEA6 uses a

Table 4
Summarized comparison results of RLHEA against the RLHEA3 and RLHEA4 variants in terms of the best and average objective values on the 54 large instances.

Instance	Pair algorithms	f_{best}				f_{avg}			
		#Wins	#Ties	#Losses	p-value	#Wins	#Ties	#Losses	p-value
Tuzun-Burke(36)	RLHEA vs. RLHEA3	3	33	0	0.11	28	4	4	1.63e-5
	RLHEA vs. RLHEA4	5	31	0	0.04	36	0	0	2.56e-6
Prodhon(18)	RLHEA vs. RLHEA3	3	15	0	0.11	12	3	3	7.55e-3
	RLHEA vs. RLHEA4	3	15	0	0.11	13	3	2	1.33e-3

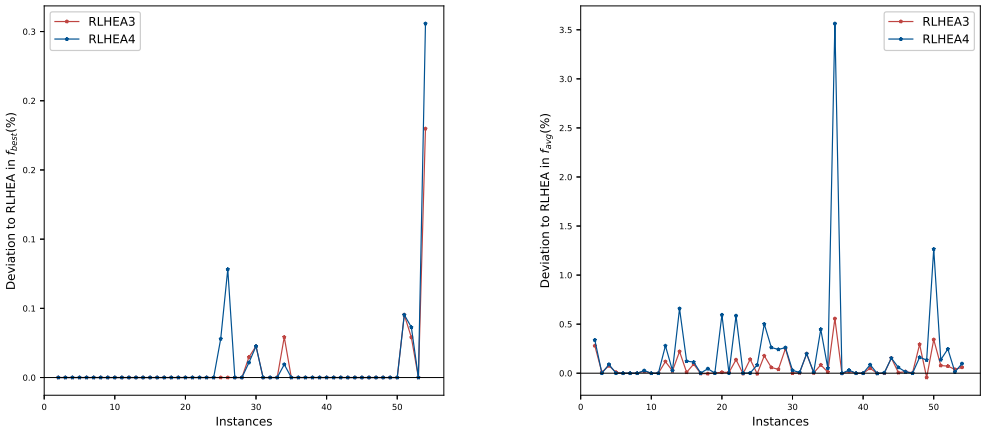

(a) Best objective value (b) Average objective value

Fig. 7. Comparative results of RLHEA with its two variants RLHEA3 and RLHEA4 on the 54 large instances.

fixed penalty parameter, which is set to the average cost per demand unit for each route of the VND input solution after the repair procedure. The summarized results of RLHEA, RLHEA5 and RLHEA6 are shown in Table 5. From the results, we can see that compared to the two variants, RLHEA, which uses strategic oscillation to balance the visit of feasible and infeasible solutions, achieves better results in terms of the best and average objective values, showing the usefulness of the strategic oscillation method.

Table 5
Summarized comparison results of RLHEA against the RLHEA5 and RLHEA6 variants in terms of the best and average objective values on the 54 selected instances.

Instance	Pair algorithms	f_{best}				f_{avg}			
		#Wins	#Ties	#Losses	p-value	#Wins	#Ties	#Losses	p-value
Tuzun-Burke(36)	RLHEA vs. RLHEA5	6	30	0	0.03	30	3	3	5.91e-6
	RLHEA vs. RLHEA6	3	33	0	0.11	26	6	4	1.24e-5
Prodhon(18)	RLHEA vs. RLHEA5	3	15	0	0.11	18	0	0	7.63e-6
	RLHEA vs. RLHEA6	2	16	0	0.18	14	2	2	1.12e-3

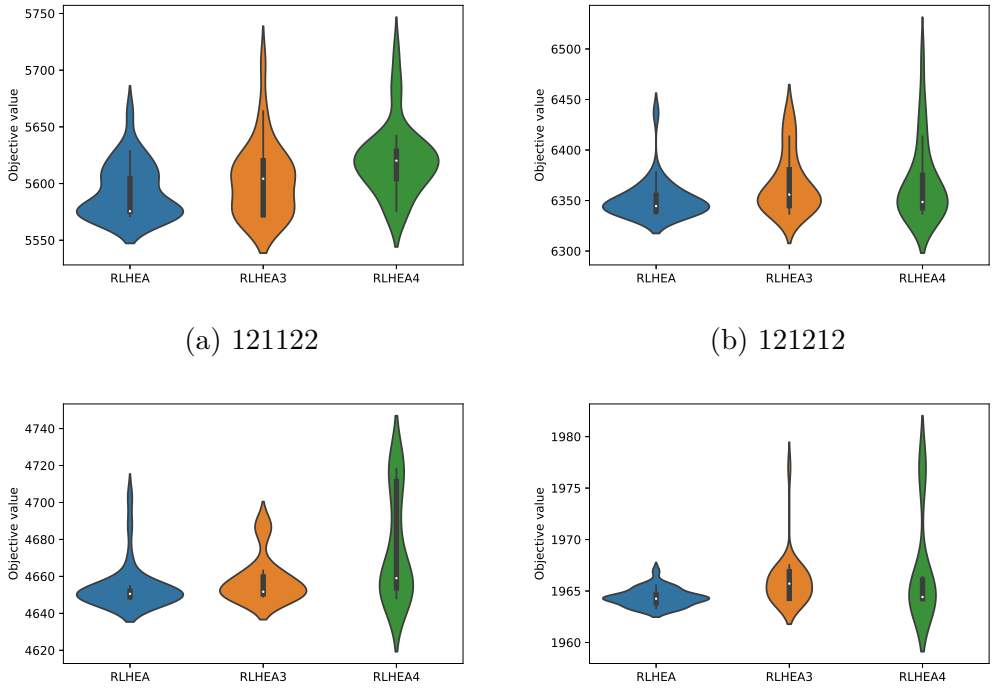

(a) 121122 (b) 121212

(c) 123122 (d) 200-10-2

Fig. 8. Violin plots of RLHEA, RLHEA3 and RLHEA4 on four instances.

5 Conclusion

The latency location routing problem is a relevant model for various real-world problems, and a number of studies have proposed methods to solve this NP-hard problem. In this study, we introduced a reinforcement learning guided hybrid evolutionary algorithm to tackle this challenging problem. The algorithm consists of three key features. Its multi-parent edge assembly crossover with three parent solutions is capable of generating promising offspring solutions while enhancing solution diversity to mitigate diversity degradation by taking route orientation into account during the crossover procedure. Its Q-learning driven variable neighborhood descent dynamically determines the exploration order of multiple neighborhoods based on knowledge learned from the search history. The use of strategic oscillation during local optimization helps to dynamically visit different feasible search spaces by traversing infeasible search spaces.

We evaluated the proposed algorithm on the 76 benchmark instances commonly used in the literature and compared it with leading algorithms. Our approach achieved 51 new best solutions while matching the best known results for the remaining instances. In addition, we performed experiments to shed light on the key components of our algorithm and reveal the rationale

behind these components.

The design principles behind the proposed algorithm are general and can be used to design effective algorithms for other problems. In particular, the idea of multi-parent edge assembly crossover is of interest for multi-route problems. The Q-learning technique used to determine the order of neighborhood exploration can contribute to the performance of local search methods that involve a portfolio of neighborhoods or search operators. Finally, the algorithm and its codes, which we will make publicly available, can be applied to practical applications related to the latency location routing problem.

Acknowledgments

We would like to thank the reviewers for their helpful comments, which helped us to improve the paper. We thank Dr. Alan Osorio-Mora and Prof. Paolo Toth, and their co-authors, for sharing the source codes of their works (Osorio-Mora et al., 2023a,b), and for their help in running the codes and answering our questions. This work was granted access to the HPC resources of the Centre Régional de Calcul Intensif des Pays de la Loire (CCIPL). Supports from the China Scholarship Council (Grant No. 202106050037) for the first author and from the National Natural Science Foundation Program of China (Grant No. 72122006) for the third author are acknowledged.

References

Aiex, R. M., Resende, M. G., & Ribeiro, C. C. (2007). Ttt plots: a perl program to create time-to-target plots. *Optimization Letters*, 1, 355–366.

Arnold, F. & Sörensen, K. (2019). What makes a vrp solution good? the generation of problem-specific knowledge for heuristics. *Computers & Operations Research*, 106, 280–288.

Glover, F. & Hao, J.-K. (2011). The case for strategic oscillation. *Annals of Operations Research*, 183, 163–173.

Hao, J.-K. (2012). Memetic algorithms in discrete optimization. *Handbook of Memetic Algorithms*, (Chapter 6, 73–94). Springer.

He, P. & Hao, J.-K. (2023a). General edge assembly crossover-driven memetic search for split delivery vehicle routing. *Transportation Science*, 57(2), 482–511.

He, P. & Hao, J.-K. (2023b). Memetic search for the minmax multiple traveling salesman problem with single and multiple depots. *European Journal of Operational Research*, 307(3), 1055–1070.

Helsgaun, K. (2000). An effective implementation of the lin–kernighan traveling salesman heuristic. *European Journal of Operational Research*, 126(1), 106–130.

Helsgaun, K. (2017). An extension of the lin-kernighan-helsgaun tsp solver for constrained traveling salesman and vehicle routing problems. *Roskilde University*.

Li, M., Hao, J.-K., & Wu, Q. (2024). A flow based formulation and a reinforcement learning based strategic oscillation for cross-dock door assignment. *European Journal of Operational Research*, 312(2), 473–492.

López-Ibáñez, M., Dubois-Lacoste, J., Cáceres, L. P., Birattari, M., & Stützle, T. (2016). The irace package: Iterated racing for automatic algorithm configuration. *Operations Research Perspectives*, 3, 43–58.

Lu, Y., Benlic, U., & Wu, Q. (2018). A hybrid dynamic programming and memetic algorithm to the traveling salesman problem with hotel selection. *Computers & Operations Research*, 90, 193–207.

Mladenović, N. & Hansen, P. (1997). Variable neighborhood search. *Computers & Operations Research*, 24(11), 1097–1100.

Moscato, P. (1999). Memetic algorithms: a short introduction. *New Ideas in Optimization*, 219–234. McGraw-Hill Ltd.

Moshref-Javadi, M. & Lee, S. (2016). The latency location-routing problem. *European Journal of Operational Research*, 255(2), 604–619.

Mühlenbein, H. (1991). Evolution in time and space–the parallel genetic algorithm. *Foundations of Genetic Algorithms*, volume 1, 316–337. Morgan Kaufmann Publisher, Inc.

Nagata, Y. (1997). Edge assembly crossover: A high-power genetic algorithm for the traveling salesman problem. *Proceedings of the 7th Internatinal Conferencen on Genetic Algorithms*, 450–457.

Nagata, Y. (2007). Edge assembly crossover for the capacitated vehicle routing problem. *7th European Conference on Evolutionary Computation in Combinatorial Optimization*, 142–153.

Nagata, Y., Bräysy, O., & Dullaert, W. (2010). A penalty-based edge assembly memetic algorithm for the vehicle routing problem with time windows. *Computers & Operations Research*, 37(4), 724–737.

Nagata, Y. & Kobayashi, S. (2013). A powerful genetic algorithm using edge assembly crossover for the traveling salesman problem. *INFORMS Journal on Computing*, 25(2), 346–363.

Ngueveu, S. U., Prins, C., & Wolfler Calvo, R. (2010). An effective memetic algorithm for the cumulative capacitated vehicle routing problem. *Computers & Operations Research*, 37(11), 1877–1885.

Nucamendi-Guillén, S., Martínez-Salazar, I., Khodaparasti, S., & Bruni, M. E. (2022). New formulations and solution approaches for the latency location routing problem. *Computers & Operations Research*, 143, 105767.

Osorio-Mora, A., Escobar, J. W., & Toth, P. (2023a). An iterated local search algorithm for latency vehicle routing problems with multiple depots. *Computers & Operations Research*, 158, 106293.

Osorio-Mora, A., Rey, C., Toth, P., & Vigo, D. (2023b). Effective metaheuristics for the latency location routing problem. *International Transactions in Operational Research*, 30, 3801–3832.

Ren, J., Hao, J.-K., Wu, F., & Fu, Z.-H. (2023). An effective hybrid search algorithm for the multiple traveling repairman problem with profits. *European Journal of Operational Research*, 304(2), 381–394.

Sanches, D., Whitley, D., & Tinós, R. (2017). Building a better heuristic for the traveling salesman problem: Combining edge assembly crossover and partition crossover. *Proceedings of the 2017 Genetic and Evolutionary Computation Conference*, 329–336.

Toth, P. & Vigo, D. (2003). The granular tabu search and its application to the vehicle-routing problem. *INFORMS Journal on Computing*, 15(4), 333–346.

Vidal, T. (2022). Hybrid genetic search for the cvrp: Open-source implementation and swap* neighborhood. *Computers & Operations Research*, 140, 105643.

Watkins, C. J. & Dayan, P. (1992). Q-learning. *Machine Learning*, 8, 279–292.

Wei, Z., Hao, J.-K., Ren, J., & Glover, F. (2023). Responsive strategic oscillation for solving the disjunctively constrained knapsack problem. *European Journal of Operational Research*, 309(3), 993–1009.

Whitley, D., Hains, D., & Howe, A. (2009). Tunneling between optima: partition crossover for the traveling salesman problem. *Proceedings of the 11th Annual Conference on Genetic and Evolutionary Computation*, 915–922.

Zhou, Q., Hao, J.-K., & Wu, Q. (2021). Responsive threshold search based memetic algorithm for balanced minimum sum-of-squares clustering. *Information Sciences*, 569, 184–204.

Zou, Y., Hao, J.-K., & Wu, Q. (2024). A two-individual evolutionary algorithm for cumulative capacitated vehicle routing with single and multiple depots. *IEEE Transactions on Evolutionary Computation*, doi:10.1109/TEVC.2024.3361910.

A Detailed comparison results

This section shows the detailed comparison results by the RLHEA algorithm and the reference algorithms, including GBILS (Nucamendi-Guillén et al., 2022), SA-VND0, SA-VND1, SA-VND2 (Osorio-Mora et al., 2023b) and M-ILS (Osorio-Mora et al., 2023a). Tables A.1 to A.3 show the comprehensive results on the three datasets, *Tuzun-Burke*, *Prodhon*, and *Barreto*, respectively. The "Instances" column presents information about each instance, including the name, number of customers N_c, number of depots N_d, and the fleet size N_v. Note that in the *Prodhon* and *Barreto* sets, the size information, such as the number of customers and depots, can be inferred from their names, so

this information is not listed separately. The "BKS" column shows the current best-known objective value for each instance reported in the literature, where underlined values are proven optimal values. The columns f_{best} and f_{avg} give the best objective value and the average value over all independent runs. T_{avg} shows the average running time in seconds. It should be noted that the running times shown for the algorithms SA-VND0, SA-VND1, SA-VND2, and M-ILS are the times observed on the same computer used for our RLHEA algorithm. To ensure a fair comparison, a scaling factor of 1.02 was applied to the running time of GBILS, based on the single-thread performance, as indicated by the machine information [2]. The best solutions among the compared results are highlighted in bold in the tables. The improved best solutions (new upper bounds) are marked with an asterisk *.

[2] https://www.cpubenchmark.net/

Table A.1
Comparative results of the RLHEA algorithm with the reference algorithms on the set *Tuzun-Burke*.

Instances					SA-VND0			SA-VND1			SA-VND2			M-ILS			RLHEA		
Name	N_c	N_d	N_v	BKS	f_{best}	f_{avg}	T_{avg}	f_{best}	f_{avg}	T_{avg}	f_{best}	f_{avg}	T_{avg}	f_{bst}	f_{avg}	T_{avg}	f_{best}	f_{avg}	T_{avg}
111112	100	10	11	3834.91	3862.86	3971.50	164.54	3892.97	3972.93	213.53	3887.86	3970.09	234.55	3834.91	3884.56	172.92	**3826.78***	3827.15	81.67
111122	100	20	11	3602.70	3612.36	3694.70	168.76	3633.60	3712.64	218.58	3602.70	3693.00	252.69	3659.46	3698.24	182.33	**3597.64***	3604.37	78.18
111212	100	10	10	3919.74	3960.24	4038.24	154.78	3988.11	4067.91	208.51	3963.34	4054.02	222.67	3919.74	3998.66	203.02	**3901.18***	3902.75	101.06
111222	100	20	11	4065.04	4086.74	4140.33	170.05	4077.87	4147.90	211.86	4065.70	4135.25	249.10	4065.04	4134.88	182.71	**4058.09***	4062.18	86.99
112112	100	10	11	2726.41	2739.16	2755.53	206.47	2740.21	2759.43	263.28	2749.48	2757.67	286.65	**2726.41**	2749.93	143.99	**2726.41**	2726.41	85.78
112122	100	20	11	2057.30	2060.29	2072.57	198.98	2057.45	2078.03	243.93	2060.29	2074.93	273.22	2057.30	2061.79	96.96	**2056.84***	2056.84	60.14
112212	100	10	12	1394.65	1402.97	1416.20	208.88	1403.57	1416.72	280.59	1404.58	1415.56	300.11	**1394.65**	1409.73	136.47	**1394.65**	1394.65	56.27
112222	100	20	11	1618.93	1623.69	1633.00	219.86	1621.40	1633.94	276.28	1625.44	1634.90	293.26	1618.93	1631.37	139.87	**1614.83***	1614.83	78.51
113112	100	10	11	2826.52	2837.51	2852.63	182.80	2835.76	2853.57	241.31	2833.66	2853.50	268.61	**2826.52**	2841.15	158.13	**2826.52**	2826.52	104.47
113122	100	20	11	2772.98	2776.39	2782.53	175.52	2774.36	2784.42	246.00	2776.39	2781.45	251.11	**2772.98**	2798.60	214.48	**2772.98**	2772.98	65.16
113212	100	10	12	1815.62	1817.00	1823.15	189.94	**1815.62**	1822.81	256.71	**1815.62**	1823.88	277.66	1817.00	1835.52	181.58	**1815.62**	1815.62	47.89
113222	100	20	11	1876.14	1876.14	1888.46	170.52	1879.63	1890.96	217.34	1878.17	1891.00	233.39	1876.58	1885.67	146.63	**1874.42***	1874.45	68.21
131112	150	10	16	5411.43	5473.18	5582.94	320.34	5464.21	5570.12	507.95	5466.75	5589.24	545.67	5411.43	5478.14	319.87	**5405.04***	5406.30	174.53
131122	150	20	16	4926.87	4993.36	5142.06	364.16	5009.26	5143.19	541.17	4967.39	5154.30	547.68	4926.87	5051.01	314.02	**4870.82***	4884.55	182.04
131212	150	10	17	5558.83	5679.70	5787.34	371.24	5606.31	5785.18	603.00	5658.71	5776.08	564.77	5558.83	5637.11	341.80	**5525.91***	5550.53	156.06
131222	150	20	17	5060.71	5141.89	5284.44	366.60	5126.95	5277.65	580.13	5166.72	5279.36	529.19	5060.71	5106.51	350.46	**5039.22***	5068.44	180.93
132112	150	10	16	3850.90	3868.88	3895.91	491.93	3883.40	3899.41	757.98	3879.81	3901.40	728.69	3850.90	3881.92	305.86	**3831.89***	3832.05	218.87
132122	150	20	16	3738.61	3740.10	3795.93	431.31	3752.76	3787.72	654.21	3768.60	3796.56	667.73	3738.61	3785.14	304.60	**3721.93***	3722.67	176.88
132212	150	10	17	2835.66	2842.10	2857.29	519.25	2837.84	2860.70	741.29	2840.11	2855.58	761.57	2835.66	2848.89	275.57	**2835.25***	2835.34	139.13
132222	150	20	17	1655.39	1660.89	1691.97	561.19	1672.86	1697.45	761.57	1669.51	1691.96	778.57	1655.39	1676.46	215.95	**1646.45***	1646.56	178.13
133112	150	10	16	4581.60	4588.38	4619.91	399.98	4598.23	4630.69	572.31	4587.35	4633.07	596.78	4581.60	4615.95	235.00	**4556.33***	4556.33	149.38
133122	150	20	16	3211.98	3223.44	3259.45	438.16	3225.56	3271.04	677.99	3227.27	3255.20	630.51	3211.98	3237.28	310.77	**3208.21***	3208.60	178.17
133212	150	10	17	2903.36	2911.58	2938.05	531.82	2911.35	2938.01	761.78	2905.45	2938.41	769.77	2903.36	2919.40	246.40	**2896.63***	2897.15	151.80
133222	150	20	17	2485.07	2502.97	2551.31	501.77	2502.68	2558.34	728.81	2507.87	2534.09	724.39	2485.07	2492.94	231.98	**2484.68***	2484.68	182.02
121112	200	10	21	6573.72	6608.45	6821.20	762.24	6621.55	6881.38	1196.02	6721.82	6894.98	1180.02	6573.72	6628.07	502.90	**6499.53***	6506.93	316.29
121122	200	20	22	5612.82	5730.53	5954.23	892.22	5788.72	5966.38	1392.03	5762.73	5935.57	1479.41	5612.82	5679.77	487.83	**5571.24***	5592.63	320.55
121212	200	10	21	6394.33	6503.36	6613.84	791.44	6429.62	6608.92	1258.20	6512.62	6643.75	1237.28	6394.33	6450.87	505.81	**6337.03***	6350.82	312.35
121222	200	20	21	6428.31	6551.73	6759.22	789.09	6562.11	6796.71	1324.77	6544.89	6769.32	1242.46	6428.31	6522.74	573.24	**6349.27***	6382.93	320.36
122112	200	10	21	6111.52	6154.64	6255.10	883.92	6184.70	6280.31	1705.19	6192.70	6274.04	1153.85	6111.52	6203.24	833.95	**6018.59***	6043.38	486.10
122122	200	20	21	3726.80	3757.37	3782.47	995.03	3757.27	3792.67	1547.20	3751.31	3786.07	1459.85	3726.80	3754.67	437.73	**3705.59***	3709.02	264.10
122212	200	10	21	4018.86	4046.81	4075.78	922.81	4046.42	4078.60	1520.92	4048.88	4082.98	1352.78	4018.86	4036.49	380.40	**4013.55***	4014.10	265.99
122222	200	20	22	2047.95	2054.32	2083.56	996.79	2052.22	2084.10	1530.59	2061.32	2081.97	1490.62	2047.95	2057.11	358.11	**2033.34***	2033.52	316.88
123112	200	10	22	4868.90	4916.97	5024.07	908.81	4967.11	5047.87	1407.80	4931.24	5019.94	1489.04	4868.90	4916.56	520.88	**4842.05***	4842.08	313.68
123122	200	20	22	4675.34	4725.91	4771.90	898.15	4707.60	4785.89	1350.76	4719.04	4761.84	1278.30	4675.34	4705.53	545.92	**4647.68***	4654.10	320.55
123212	200	10	22	5135.21	5170.77	5218.43	868.24	5178.02	5225.04	1351.98	5183.34	5259.76	1172.57	5135.21	5174.88	332.78	**5123.41***	5124.13	262.12
123222	200	20	22	2528.74	2567.20	2629.66	876.49	2555.18	2633.86	1363.16	2562.46	2602.87	1353.88	2528.74	2557.17	344.07	**2494.58***	2494.58	263.87

Table A.2
Comparative results of proposed RLHEA with the reference algorithms on the set *Prodhon*.

Instances			GBILS		SA-VND0			SA-VND1			SA-VND2			M-ILS			RLHEA		
Name	N_v	BKS	f_{best}	T_{avg}	f_{best}	f_{avg}	T_{avg}	f_{best}	f_{avg}	T_{avg}	f_{best}	f_{avg}	T_{avg}	f_{bst}	f_{avg}	T_{avg}	f_{best}	f_{avg}	T_{avg}
20-5-1	5	330.00	**330.00**	0.34	**330.00**	330.00	9.85	**330.00**	330.00	8.59	**330.00**	330.00	13.11	**330.00**	330.00	13.92	**330.00**	330.00	3.23
20-5-1b	3	608.05	**608.06**	0.15	**608.05**	608.06	11.56	**608.05**	608.06	8.80	608.05	608.06	19.98	615.66	615.66	10.10	**608.05**	608.06	3.57
20-5-2	5	301.97	**301.97**	0.24	**301.97**	301.97	8.31	**301.97**	301.97	7.28	**301.97**	301.97	12.27	**301.97**	301.97	13.64	**301.97**	301.97	3.76
20-5-2b	3	486.55	**486.55**	0.25	**486.55**	486.55	12.31	**486.55**	486.55	10.23	**486.55**	486.55	20.68	**486.55**	486.55	10.10	**486.55**	486.54	3.69
50-5-1	12	843.93	846.88	50.32	846.17	849.77	59.10	846.51	850.10	58.17	844.63	849.66	69.99	**843.93**	845.75	48.57	**843.93**	843.93	15.71
50-5-1b	6	1293.46	**1293.93**	21.46	**1293.46**	1293.71	46.72	**1293.46**	1293.54	44.53	**1293.46**	1293.48	73.74	**1293.46**	1293.95	58.81	**1293.46**	1293.46	20.90
50-5-2	12	684.13	691.67	38.49	**684.13**	693.78	48.30	**684.13**	692.43	60.38	**684.13**	697.61	59.33	**684.13**	690.69	73.43	**684.13**	684.13	15.72
50-5-2b	6	953.25	954.88	22.44	**953.25**	953.50	39.05	**953.25**	953.35	39.71	**953.25**	953.40	63.61	**953.25**	953.68	48.90	**953.25**	953.25	16.73
50-5-2BIS	12	945.45	952.55	39.56	949.13	950.80	65.24	949.57	951.13	83.25	949.56	951.46	73.98	**945.45**	945.65	121.85	**945.45**	945.45	12.14
50-5-2bBIS	6	803.90	**803.90**	31.67	**803.90**	803.90	49.70	**803.90**	803.90	48.13	**803.90**	803.90	68.76	**803.90**	803.90	54.99	**803.90**	803.90	13.73
50-5-3	12	831.57	832.15	39.09	831.97	835.10	53.74	833.01	834.91	62.43	833.01	836.25	69.43	**831.57**	834.30	81.44	**831.57**	831.57	18.37
50-5-3b	6	1101.57	1106.57	22.75	**1101.57**	1103.15	39.30	**1101.57**	1103.94	41.72	**1101.57**	1102.47	61.71	**1101.57**	1102.49	37.31	**1101.57**	1101.57	19.59
100-5-1	24	2000.80	2035.60	21.24	2004.33	2023.35	246.05	2010.49	2023.78	378.85	2016.44	2028.27	307.25	2000.80	2012.06	184.89	**1997.29***	1997.37	63.14
100-5-1b	12	2311.01	2357.87	33.69	2311.84	2336.64	182.67	2312.53	2337.27	227.13	2317.42	2336.82	252.54	2311.01	2346.47	171.41	**2305.65***	2305.89	68.43
100-5-2	24	1128.12	1144.70	26.60	1132.36	1135.99	214.42	1129.83	1135.49	343.26	1132.68	1136.61	282.63	1128.12	1133.17	198.13	**1126.39***	1126.39	65.69
100-5-2b	11	1507.88	1567.44	31.73	1507.88	1517.11	205.25	1510.57	1519.04	247.41	1510.24	1519.44	271.72	1507.88	1511.89	119.62	**1506.79***	1506.79	84.88
100-5-3	24	1572.61	1596.77	16.12	1581.93	1587.20	219.07	1581.93	1586.49	344.91	1579.38	1587.41	283.76	1572.61	1582.05	233.51	**1567.62***	1568.22	59.34
100-5-3b	11	1933.70	2032.13	37.66	1933.70	1950.89	180.90	1935.70	1953.85	258.79	1940.47	1955.56	255.64	1934.93	1954.50	163.38	**1932.96***	1933.07	73.12
100-10-1	26	1458.80	1481.56	26.33	1472.85	1511.00	247.27	1470.71	1503.92	371.15	1461.53	1513.44	333.90	1458.80	1464.80	196.75	**1457.53***	1457.68	59.80
100-10-1b	12	1899.80	1984.91	33.05	1901.27	1953.96	193.46	1915.77	1972.26	253.50	1926.32	1963.33	255.59	1899.80	1918.20	186.81	**1894.92***	1895.83	63.40
100-10-2	24	1137.59	1287.50	24.84	1143.30	1152.81	251.82	1142.31	1155.47	370.05	1141.45	1156.81	332.11	1137.59	1144.99	233.59	**1134.80***	1135.23	48.99
100-10-2b	11	1559.88	1645.07	45.62	1566.48	1585.67	195.28	1566.48	1588.24	256.10	1568.71	1583.06	267.51	1559.88	1570.80	190.30	**1555.71***	1555.71	58.02
100-10-3	25	1204.94	1216.20	18.76	1209.20	1221.52	277.89	1209.86	1225.98	376.80	1210.61	1225.49	352.77	1204.94	1209.27	151.09	**1204.01***	1204.01	56.63
100-10-3b	11	1653.83	1745.05	22.99	1662.43	1705.63	187.74	1665.69	1706.68	243.04	1676.25	1705.51	262.94	1653.83	1670.95	196.73	**1647.85***	1649.38	67.45
200-10-1	49	2780.03	2861.85	91.20	2798.57	2854.10	1327.81	2797.86	2863.27	2204.55	2792.24	2860.29	2026.86	2780.03	2788.95	568.99	**2770.45***	2774.33	240.31
200-10-1b	22	3290.73	3557.96	99.69	3368.71	3477.07	956.22	3355.70	3478.91	1572.79	3327.76	3456.43	1411.39	3290.73	3336.49	522.54	**3270.68***	3292.13	249.43
200-10-2	49	1973.41	1997.01	112.28	1984.96	2001.97	1164.73	1986.55	2004.51	2571.48	1986.51	2003.80	1853.75	1973.41	1980.50	429.89	**1963.32***	1964.37	206.21
200-10-2b	23	2328.12	2473.24	89.74	2336.11	2379.01	932.35	2355.15	2378.21	1704.98	2336.29	2377.63	1453.02	2328.12	2360.59	438.38	**2309.30***	2314.74	174.98
200-10-3	48	2727.15	2783.20	106.18	2741.16	2758.09	1075.86	2744.67	2757.42	2293.23	2750.18	2762.07	1612.10	2727.15	2736.47	419.99	**2719.34***	2720.27	182.54
200-10-3b	22	3194.53	3413.34	92.27	3242.18	3274.58	772.47	3233.89	3267.81	1422.02	3225.11	3272.52	1226.53	3194.53	3220.29	345.12	**3174.91***	3186.06	183.21

Table A.3
Comparative results of proposed RLHEA with the reference algorithms on the set *Barreto*.

Instances			GBILS		SA-VND0			SA-VND1			SA-VND2			M-ILS			RLHEA		
Name	N_v	BKS	f_{best}	T_{avg}	f_{best}	f_{avg}	T_{avg}	f_{best}	f_{avg}	T_{avg}	f_{best}	f_{avg}	T_{avg}	f_{bst}	f_{avg}	T_{avg}	f_{best}	f_{avg}	T_{avg}
Christ_50_5	6	1661.64	1719.89	11.99	**1661.64**	1662.06	46.25	**1661.64**	1662.13	42.96	**1661.64**	1662.13	64.7	**1661.64**	1669.05	51.88	**1661.64**	1661.64	18.65
Christ_75_10	9	2370.73	2399.28	51.12	2403.79	2459.03	96.45	2383.04	2457.45	122.18	2400.86	2459.58	128.00	2370.73	2417.28	127.97	**2362.48***	2362.48	40.98
Christ_100_10	8	3791.98	3984.05	148.17	3791.98	3831.18	177.42	3806.39	3838.89	198.76	3797.00	3826.81	231.22	3803.5	3848.63	168.75	**3788.96***	3788.96	92.92
Gaskell_21_5	4	653.48	**653.48**	0.28	**653.48**	653.48	9.33	**653.48**	653.48	8.67	**653.48**	653.48	13.86	**653.48**	653.48	11.93	**653.48**	653.48	4.06
Gaskell_29_5	4	1199.33	**1199.33**	1.70	**1199.33**	1199.33	25.33	**1199.33**	1199.33	21.29	**1199.33**	1199.33	40.27	**1199.33**	1199.33	22.26	**1199.33**	1199.33	7.30
Gaskell_32_5b	3	1552.84	**1552.84**	1.60	**1552.84**	1553.29	35.58	**1552.84**	1553.29	27.65	**1552.84**	1552.84	55.69	**1552.84**	1556.58	24.35	**1552.84**	1552.84	9.00
Gaskell_36_5	4	1627.17	**1627.17**	1.05	**1627.17**	1627.17	25.76	**1627.17**	1627.17	22.72	**1627.17**	1627.17	39.59	**1627.17**	1628.12	29.56	**1627.17**	1627.17	11.26
Min_27_5	4	5387.55	**5387.55**	27.55	**5387.55**	5387.55	14.27	**5387.55**	5387.55	12.25	**5387.55**	5387.55	22.73	**5387.55**	5387.55	10.59	**5387.55**	5387.55	5.98
Min_134_8	11	21751.97	-	-	21852.35	22307.28	194.27	21910.54	22309.19	215.35	21853.52	22256.20	276.15	**21751.97**	22450.39	164.69	**21751.97**	21751.97	131.91
Or_117_14	7	53798.53	-	-	**53798.53**	54866.72	108.95	53859.08	54805.87	105.50	54103.16	54902.35	171.64	54328.75	56687.87	125.96	**53798.53**	53907.31	97.84